Published in final edited form as:
Circulation. 2011 September 13; 124(11): 1212–1222. doi:10.1161/CIRCULATIONAHA.111.023986.

Defects in ankyrin-based membrane protein targeting pathways underlie atrial fibrillation

Shane R. Cunha, Ph.D.[1,5], **Thomas J. Hund, Ph.D.**[1,2,4], **Seyed Hashemi, M.D.**[6], **Niels Voigt, M.D.**[8], **Na Li, M.D.**[10], **Patrick Wright, B.S.**[1], **Olha Koval, Ph.D.**[6], **Jingdong Li, M.D.**[1], **Hjalti Gudmundsson, M.D.**[6], **Richard J. Gumina, M.D., Ph.D.**[1,2], **Matthias Karck, M.D.**[9], **Jean-Jacques Schott, Ph.D.**[11], **Vincent Probst, M.D., Ph.D.**[11], **Herve Le Marec, M.D., Ph.D.**[11], **Mark E. Anderson, M.D., Ph.D.**[6,7], **Dobromir Dobrev, M.D.**[8], **Xander HT Wehrens, M.D., Ph.D.**[10], and **Peter J Mohler, Ph.D.**[1,2,3]

[1]Dorothy M. Davis Heart and Lung Research Institute, The Ohio State University Medical Center, Columbus, OH

[2]Departments of Internal Medicine, Division of Cardiovascular Medicine, Physiology & Cell Biology, and Biomedical Engineering, The Ohio State University Medical Center, Columbus, OH

[3]Departments of Internal Medicine, Division of Cardiovascular Medicine, Physiology & Cell Biology, and Biomedical Engineering, The Ohio State University Medical Center, Columbus, OH

[4]Departments of Internal Medicine, Division of Cardiovascular Medicine, Physiology & Cell Biology, and Biomedical Engineering, The Ohio State University Medical Center, Columbus, OH

[5]Department of Integrative Biology and Pharmacology, University of Texas Health Science Center, Houston, TX

[6]Departments of Internal Medicine and Molecular Physiology & Biophysics, University of Iowa Carver College of Medicine, Iowa City, IA

[7]Departments of Internal Medicine and Molecular Physiology & Biophysics, University of Iowa Carver College of Medicine, Iowa City, IA

[8]Division of Experimental Cardiology, Medical Faculty Mannheim, University of Heidelberg, Mannheim, Germany

[9]Department of Cardiac Surgery, University of Heidelberg, Heidelberg, Germany

[10]Departments of Molecular Physiology & Biophysics and Medicine, Baylor College of Medicine, Houston, TX

[11]INSERM, UMR915 and Universite' de Nantes, l'institut du thorax, Nantes, France

Abstract

Background—Atrial fibrillation (AF) is the most common cardiac arrhythmia, affecting over two million patients in the US alone. Despite decades of research, surprisingly little is known

Address for correspondence: Peter J Mohler, Ph.D. Dorothy M. Davis Heart and Lung Research Institute The Ohio State University Medical Center 473 W. 12th Avenue, 110G DHLRI Columbus, OH 43210 Phone: 614-292-5019 Fax: 614-247-7799 peter.mohler@osumc.edu .

Disclosures None

regarding the molecular pathways underlying the pathogenesis of AF. *ANK2* encodes ankyrin-B, a multifunctional adapter molecule implicated in membrane targeting of ion channels, transporters, and signaling molecules in excitable cells.

Methods and Results—Here, we report early-onset AF in patients harboring loss-of-function mutations in *ANK2*. In mice, we show that ankyrin-B-deficiency results in atrial electrophysiological dysfunction and increased susceptibility to AF. Moreover, ankyrin-$B^{+/-}$ atrial myocytes display shortened action potentials, consistent with human AF. Ankyrin-B is expressed in atrial myocytes, and we demonstrate its requirement for the membrane targeting and function of a subgroup of voltage-gated Ca^{2+} channels ($Ca_v1.3$) responsible for low-voltage activated L-type Ca^{2+}current. Ankyrin-B directly associates with $Ca_v1.3$, and this interaction is regulated by a short, highly-conserved motif specific to $Ca_v1.3$. Moreover, loss of ankyrin-B in atrial myocytes results in decreased $Ca_v1.3$ expression, membrane localization, and function sufficient to produce shortened atrial action potentials and arrhythmias. Finally, we demonstrate reduced ankyrin-B expression in atrial samples of patients with documented AF, further supporting an association between ankyrin-B and AF.

Conclusions—These findings support that reduced ankyrin-B expression or mutations in *ANK2* are associated with atrial fibrillation. Additionally, our data demonstrate a novel pathway for ankyrin-B-dependent regulation of $Ca_v1.3$ channel membrane targeting and regulation in atrial myocytes.

Keywords

Ankyrin; atrial fibrillation; calcium channel; ion channel targeting

---

Atrial fibrillation (AF), which is characterized by rapid and irregular activation of the atrium, is the most common sustained arrhythmia found in clinical practice, affecting ~2.3 million people in the US alone.[1] The prevalence of AF increases with age with ~2-6% of people over the age of 65 exhibiting AF.[2, 3] Given the demographics of the US, it is predicted that there will be a five-fold increase in the prevalence of AF by 2050.[4] While AF is frequently associated with other cardiac disorders including coronary artery disease, mitral valve disease, congenital heart disease, and congestive heart failure, ~30% of all AF cases are described as lone AF where patients exhibit no previous cardiac pathology.[5] The majority of monogenic AF cases described to date are linked to mutations that affect potassium channels, although these cases represent only a small fraction of total monogenic AF cases.[6]

Ankyrin-B (AnkB, encoded by *ANK2*) is an adapter protein expressed in a number of excitable cells including neurons, cardiomyocytes, and pancreatic beta cells.[7] Given that AnkB targets select ion channels, transporters, and signaling molecules to specific membrane domains, it is not surprising that dysfunction in the AnkB cellular pathway has been linked to neuronal defects, ventricular arrhythmia, and neonatal diabetes.[8-10]

Here, we demonstrate a critical role for AnkB in atrial function. Individuals harboring loss-of-function mutations in *ANK2* developed early-onset AF. AnkB deficient mice phenocopy *ANK2*-based human disease and displayed striking susceptibility to AF. Primary atrial myocytes from AnkB deficient mice displayed shortened action potentials, a hallmark of AF and this decrease was associated with loss of L-type Ca^{2+} current ($I_{Ca,L}$). Our data revealed that $Ca_v1.3$ is a novel AnkB-binding partner and the structural requirements for AnkB/$Ca_v1.3$ association were mapped. Specifically, a unique C-terminal motif in $Ca_V1.3$ was found to be necessary and sufficient for ankyrin-binding. In $AnkB^{+/-}$ atrial myocytes, $Ca_v1.3$ protein expression and membrane function were reduced. Moreover, we demonstrated that AnkB levels are reduced in human AF, providing an association between

AnkB and the pathogenesis of AF. Together, our data describe a novel mechanism for $Ca_v1.3$ membrane targeting in primary atrial cardiomyocytes and reveal a potential molecular mechanism underlying ankyrin-associated AF.

Methods

Immunofluorescence

Myocytes were washed with phosphate-buffered saline (PBS, pH 7.4) and fixed in warm 2% paraformaldehyde (37°C). Cells were blocked/permeabilized in PBS containing 0.075% Triton X-100 and 3% fish oil gelatin (Sigma), and incubated in primary antibody overnight at 4° C. Following washes (PBS +0.1% Triton X-100), cells were incubated in secondary antibody (Alexa 488, 568; and ToPro-3AM 633) for 8 hours at 4°C and mounted using Vectashield (Vector). Images were collected on Zeiss 510 Meta confocal microscope (40 power oil 1.40 NA, pinhole equals 1.0 Airy disc) using Zeiss Imaging software. Images were imported into Adobe Photoshop for cropping and linear contrast adjustment. Imaging experiments were performed at least three times for each experimental protocol, and >20 myocytes were examined from each experimental set.

Immunoblots

Protein lysates were isolated from atria and ventricles of WT and heterozygous ankyrin-B mice as described.[11] Antibodies and tissues are described in the online-only Data Supplement.

Cellular electrophysiology

Membrane currents and action potentials were measured with an Axon 200B patch-clamp amplifier controlled by a personal computer using a Digidata 1320A acquisition board driven by pClamp 8.0 software (Axon Instruments). Electrophysiological recordings were only obtained from Ca^{2+}-tolerant, rod-shaped atrial cells. We used perforated (amphotericin B) patch for calcium current and action potential studies. All experiments were conducted at room temperature, unless otherwise noted. Other currents were measured as described.[12] Recording pipettes, fabricated from borosilicate glass, had resistance of 2–4 MΩ, when filled with recording solution. All solutions were adjusted to 275–295 mOsm.

Statistics

For human data, differences between group means were compared by unpaired Student's *t*-test. Frequency-data were analyzed with Fisher's exact test. The Kolmogorov-Smirnov test was used to test whether data follow a normal distribution. Assumption of equal variance per group was confirmed using Bartlett's test. Data are mean±SEM. $P<0.05$ was considered statistically significant. For non-human data, all values are presented as mean ± SEM. P values were assessed with a paired Student's *t* test (two-tailed) or ANOVA, as appropriate, for continuous data. The Bonferroni test was used for post-hoc testing. The null hypothesis was rejected for $P < 0.05$.

Human tissue samples

Human tissue experimental protocols were approved by the ethics committee of the Medical Faculty Mannheim, University of Heidelberg (#2011-216N-MA). Each patient gave written informed consent. During routine cannulation procedures in patients undergoing open-heart surgery for cardiac bypass grafting and valve replacement, respectively, the tip of the right atrial appendage was removed and immediately snap-frozen in liquid nitrogen. Appendages were obtained from 12 sinus rhythm (SR) and 10 paroxysmal atrial fibrillation (pAF, Supplemental Table 2 in the on-line only Data Supplement) patients. The AF group included

patients in sinus rhythm at surgery with a history of at least one episode of self-terminating AF lasting less than 7 days (pAF patients).

Additional Methods are presented in the online-only Data Supplement.

Results

Ankyrin-B dysfunction is associated with human atrial fibrillation

We identified a high incidence of AF in *ANK2* mutation-positive probands. Probands harboring *ANK2* loss-of-function alleles displayed early onset AF, commonly progressing to permanent AF.[9, 13, 14] In one large kindred (74 members), 13 of 25 *ANK2* loss-of-function variant carriers (phenotypes previously mapped to *ANK2*, Z_{max}=7.05[9]) displayed AF (mean onset 40 ±18 years, 5 paroxysmal, 8 permanent), whereas non-carriers were asymptomatic. Only two individuals were non-penetrant for atrial phenotypes. The others had AF, AF with sinus node dysfunction, or sinus node dysfunction alone. In an unrelated large family, 20/36 individuals were positive for the *ANK2* disease allele (maximal LOD score was for marker D4S1616; linkage Z_{max}=5.9, θ=0), and 3 of 20 disease allele carriers displayed AF (mean onset 48 ±12 years, two paroxysmal, 1 permanent), while thirteen displayed sinus node disease requiring pacemaker implantation (mean age for implantation 30±18 years[12]). Only four individuals were non-penetrant for atrial phenotypes. In addition to AF, prior work demonstrates that *ANK2* variant carriers may display prolonged ventricular QT intervals, which predisposes individuals to ventricular arrhythmias (examples of cardiac phenotypes are presented in Supplemental Table 1 in the on-line only Data Supplement).[9, 13] As AF and long QT syndrome (LQTS) are often associated with opposing action potential characteristics (i.e., AF with shortened atrial action potentials; LQTS with prolonged ventricular action potentials), we hypothesized that AnkB might uniquely affect atrial ion channels resulting in an increased susceptibility to AF.

Mice deficient for ankyrin-B expression display atrial dysfunction

Previous studies have demonstrated that human *ANK2* gene mutations linked with arrhythmia behave as loss-of-function when analyzed in primary cardiomyocytes.[9, 12-14] Therefore, we assessed the role of AnkB deficiency in atria of mice heterozygous for a null mutation in AnkB ($AnkB^{+/-}$ mice, as $AnkB^{-/-}$ mice die at birth). Continuous telemetry ECG recordings from conscious $AnkB^{+/-}$ mice revealed atrial arrhythmias also present in human carriers of *ANK2* variants, including spontaneous bradycardia with erratic atrial activity, lack of discrete P waves and variable ventricular response (Figure 1A-D).

We next tested the susceptibility to atrial arrhythmias in $AnkB^{+/-}$ mice following atrial burst pacing.[15] Intracardiac electrograms were recorded simultaneously with the surface ECG to confirm the nature of abnormal atrial electrical activities. Periods of pacing-induced AF were observed in the majority (~75%) of $AnkB^{+/-}$ mice (11/15 mice; Figure 1E-F). In contrast, a significantly lower fraction of WT mice demonstrated AF inducibility using this protocol (2/9 WT mice, $p<0.05$ vs. $AnkB^{+/-}$; Figure 1F). $AnkB^{+/-}$ atrial episodes showed characteristic absence of P waves and RR interval variability.[15] Moreover, atrial fibrillation/tachycardia was confirmed by the presence of rapid and irregular A waves on the atrioventricular electrogram (Figure 1E). Together, the electrophysiological data in human *ANK2* mutation carriers and $AnkB^{+/-}$ mice clearly demonstrate that AnkB dysfunction is detrimental for normal atrial electrical activity.

Ankyrin-B is expressed in atria

We used immunoblot to identify AnkB expression patterns in human atria. AnkB was expressed in all human heart chambers at similar levels (Figure 2A). As expected, voltage-

gated calcium channel $Ca_v1.2$ was most abundant in the right and left ventricle, whereas $Ca_v1.3$ was enriched in right and left atria compared with ventricle[16] (Figure 2A). At the level of the single atrial cardiomyocyte, AnkB was present at both the peripheral sarcolemma (yellow arrows) as well as the M-line (Figure 2B, white arrows). These data demonstrate that AnkB is expressed in atrial tissue and localized at select membrane domains in isolated primary atrial cells.

Ankyrin-B$^{+/-}$ atrial myocytes display aberrant atrial electrical activity

To define the role of AnkB in atria, we evaluated action potentials from isolated WT and AnkB$^{+/-}$ atrial cardiomyocytes. Notably, AnkB$^{+/-}$ atrial myocytes displayed significantly reduced action potential durations (measured at 90% of repolarization, APD_{90}) compared with WT atrial cardiomyocytes (Figure 2C-D). In fact, APD90 was reduced ~25% in AnkB$^{+/-}$ atrial cardiomyocytes at both room (Figure 2C-D, n=7 WT, n=8 AnkB$^{+/-}$, $p<0.05$) and physiological temperature (Supplemental Figure 1 in the on-line only Data Supplement, n=6 WT, n=5 AnkB$^{+/-}$, $p<0.05$), a cellular phenotype consistent with that observed in AF patients.[17] In contrast, prior studies revealed that AnkB$^{+/-}$ ventricular cardiomyocytes do not display significant differences in APD_{90} compared to WT.[9]

Atrial myocyte depolarization and repolarization is regulated by the synchronized activities of membrane-associated ion channels, transporters, and pumps. To define the molecular basis of action potential shortening in AnkB$^{+/-}$ atrial myocytes, we investigated the activities of a number of critical atrial myocyte currents. We observed a significantly reduced $I_{Ca,L}$ in AnkB$^{+/-}$ atrial myocytes (Figure 2E-F, n=7 WT, n=8 AnkB$^{+/-}$, $p<0.05$) in contrast to AnkB$^{+/-}$ ventricular myocytes that display normal $I_{Ca,L}$ and APD.[9] We observed no difference in I_{Na} (Figure 2G-H, n=7 WT, n=8 AnkB$^{+/-}$, N.S.), total I_K, or I_{to} between WT and AnkB$^{+/-}$ atrial myocytes (n=7 WT, n=8 AnkB$^{+/-}$; N.S.; not shown). However, we did observe a significant decrease in I_{NCX}, consistent with previous findings in AnkB-deficient ventricular myocytes (Supplemental Figure 2 in the online-only Data Supplement, n=8 WT, n=8 AnkB$^{+/-}$, $p<0.05$).[18] Thus, atrial AnkB$^{+/-}$ myocytes display decreased APD and reduced $I_{Ca,L}$. Both phenotypes are unique to AnkB$^{+/-}$ atrial cells compared with ventricular myocytes.

Reduced $Ca_v1.3$ expression in ankyrin-B$^{+/-}$ atria

In atrial myocytes, $I_{Ca,L}$ is comprised of the combined activities of $Ca_v1.2$ (α1C) and $Ca_v1.3$ (α1D). Based on reduced $I_{Ca,L}$ AnkB$^{+/-}$ in AnkB^{+-} atrial cardiomyocytes, we examined the expression and localization of both $Ca_v1.2$ and $Ca_v1.3$ in WT and AnkB$^{+/-}$ mouse atria. Consistent with electrophysiological data, we observed a significant decrease in $Ca_v1.3$ expression in AnkB$^{+/-}$ atria (reduced ~30%, n=3, $p<0.05$; Figure 3A-B), whereas $Ca_v1.2$ expression was unchanged between genotypes (Figure 3A-B, p=N.S.). Furthermore, in agreement with our earlier studies in ventricle[9, 19], $Na_v1.5$ expression levels were not altered in AnkB$^{+/-}$ atrial cells (Figure 3A). Immunofluorescence of individual atrial myocytes using channel-specific antibodies demonstrated that $Ca_v1.3$, but not $Ca_v1.2$, $Ca_v3.1$, or $Na_v1.5$ membrane expression was reduced (Figure 3C-F). In fact, we observed a ~40% decrease in membrane staining intensity for $Ca_v1.3$ in AnkB$^{+/-}$ atrial cardiomyocytes compared with WT cells (Figure 3E, $p<0.05$; n=5 WT, n=6 AnkB$^{+/-}$).

As a final test to assess AnkB function in $Ca_v1.3$ membrane targeting, we evaluated $Ca_v1.3$ membrane activity in primary cardiac fibroblasts from WT and AnkB$^{-/-}$ (homozygous null) mice (harvested before death of AnkB$^{-/-}$ neonatal mice). Primary fibroblasts were chosen to allow recording of $I_{Ca,L}$ from exogenously expressed $Ca_v1.3$ without confounding native current from endogenous Ca^{2+} channels (note that WT and AnkB$^{-/-}$ primary fibroblasts display little endogenous I_{Ca}, open circles in Figure 3G). As expected, WT fibroblasts

expressing $Ca_v1.3$ displayed significantly greater $I_{Ca,L}$ compared with non-transfected cells (Figure 3G, n=9 WT, n=7 AnkB+/− cells, $p<0.05$). In contrast, $AnkB^{-/-}$ primary cells expressing $Ca_v1.3$ showed >50% reduction in $I_{Ca,L}$ (Figure 3G; n=9 WT, n=7 AnkB+/− cells, $p<0.05$) and reduced $Ca_v1.3$ membrane immunofluorescence (Figure 3H) compared to WT cells, despite similar $Ca_v1.3$ protein expression in both cell types (based on immunoblot). These phenotypes were directly related to AnkB expression, as exogenous AnkB expression restored $I_{Ca,L}$ levels in $AnkB^{-/-}$ cells (Figure 3I-J, n=8, $p<0.05$). Notably, in contrast to $Ca_v1.3$, we observed no functional difference in $Ca_v1.2$ membrane expression between wild-type and ankyrin-B-deficient cells (Supplemental Figure 3A-B in the online-only Data Supplement, n=5 WT, n=6 $AnkB^{+/-}$; N.S.).

Ankyrin-B directly associates with $Ca_v1.3$

Based on electrophysiological data from primary myocytes and fibroblasts showing reduced $Ca_v1.3$ in AnkB-deficient atrial myocytes, we tested for a direct interaction between AnkB and $Ca_v1.3$. Full-length $Ca_v1.3$ has five major cytoplasmic domains including an amino terminal domain, three cytoplasmic segments that connect the four major transmembrane regions (DI-DIV), and a large C-terminal domain (Figure 4A). We generated radiolabeled purified protein of each $Ca_v1.3$ cytoplasmic region (N1, L1-L3, C1-C4). Due to the extensive length of the C-terminal domain, this region was further subdivided into four segments for direct binding experiments (Figure 4A, C1-C4). We observed significant association between GST-labeled AnkB membrane-binding domain and only one intracellular region of $Ca_v1.3$, the C4 region of the C-terminus (residues 2014-2203; Figure 4B). This interaction was specific to AnkB, as it was not observed for the similar ankyrin-G (AnkG) membrane-binding domain or GST alone (Figure 4B). These data support a direct and specific interaction between AnkB membrane-binding domain and the C-terminal domain of $Ca_v1.3$.

While our functional data suggested a specific interaction of AnkB with $Ca_v1.3$, $Ca_v1.2$ and $Ca_v1.3$ share significant sequence similarity in the distal C-terminal regions (residues 2014-2203 of $Ca_v1.3$; Figure 4C). We therefore tested for the interaction of the AnkB membrane-binding domain with both $Ca_v1.2$ and $Ca_v1.3$ C-terminal domains (residues 1958-2159 of $Ca_v1.2$). Consistent with our previous imaging, biochemical, and functional data, we observed no interaction of AnkB or AnkG with the $Ca_v1.2$ C-terminal domain (Figure 4D).

The $Ca_v1.3$, but not $Ca_v1.2$ C-terminal domain contains a short motif resembling the ankyrin-binding sequence found in voltage-gated Na_v channels (i.e. $Na_v1.2$, $Na_v1.5$) and inwardly rectifying K^+ channels (i.e. Kir6.2; Figure 4E).[8, 20, 21] Importantly, this sequence is conserved across $Ca_v1.3$ orthologues (Figure 4F). We tested the requirement of this motif for AnkB-binding using a mutant C-terminal domain lacking these residues (see Figure 4G). While $Ca_v1.3$ C-terminal domain associated with AnkB (but not AnkG), $Ca_v1.3$ C4 ΔABD lacking the putative ankyrin-binding domain failed to associate with AnkB (Figure 4H). Based on these results, we tested whether residues 2175-2198 were sufficient for ankyrin-binding using biotinylated peptides. We observed an association of full-length endogenous AnkB from human atrial lysates with an immobilized peptide containing the AnkB-binding domain in $Ca_v1.3$ (Figure 4I-J). We observed no interaction with a peptide of the corresponding region in $Ca_v1.2$, or with streptavidin beads alone (Figure 4J). Together, our data demonstrate that $Ca_v1.3$ residues 2175-2198 are necessary and sufficient for direct AnkB association.

To test whether $Ca_v1.3$ membrane expression requires a direct interaction with AnkB, we measured $I_{Ca,L}$ in primary cardiac fibroblasts expressing wild-type $Ca_v1.3$ and a mutant $Ca_v1.3$ lacking the ankyrin-binding motif. As expected, wild-type $Ca_v1.3$ expression

resulted in robust $I_{Ca,L}$ in primary cells (Figure 4K, n=7, $p<0.05$). In contrast, $Ca_v1.3\Delta2174$ lacking the AnkB-binding motif displayed greater than 50% reduction in membrane activity compared to the WT channel (Figure 4K, n=7, $p<0.05$). These data support the requirement of a direct AnkB interaction for $Ca_v1.3$ membrane targeting. However, these data also suggest that an ankyrin-independent pathway(s) also plays a critical role in $Ca_v1.3$ membrane delivery, as $Ca_v1.3$ lacking ankyrin-binding still displayed a greatly reduced, but detectable current.

Loss of $I_{Ca,L}$ alters APD90 in ankyrin-$B^{+/-}$ atrial myocytes

Our results identify a direct association of AnkB with $Ca_v1.3$ and a striking reduction of $Ca_v1.3$ and $I_{Ca,L}$ in primary AnkB$^{+/-}$ atrial cardiomyocytes. To test whether observed differences in $I_{Ca,L}$ in AnkB$^{+/-}$ atrial myocytes are sufficient to account for dramatic action potential shortening and atrial fibrillation susceptibility, we performed computational modeling of WT and AnkB$^{+/-}$ atrial action potentials (Figure 5). We first incorporated experimentally measured changes in $I_{Ca,L}$ (Figure 2), I_{NCX} (Supplemental Figure 2 in online-only Data Supplement), as well as reduction in Na/K ATPase expression[12, 22] into a physiological and well-validated model of the atrial action potential from Nattel and colleagues.[23] Decreasing all three currents was sufficient to reduce the action potential nearly 25%, similar to the observed differences in APDs between AnkB$^{+/-}$ and WT atrial myocytes (Figure 5B, G). We next simulated action potentials in atrial myocytes deficient in NCX, Na/K ATPase, or $I_{Ca,L}$ and compared APDs to that in the WT model (Figure 5K). Reduction of $I_{Ca,L}$ alone shortened APD by nearly the same amount as observed in the AnkB$^{+/-}$ model, indicating that loss of $I_{Ca,L}$ is the dominant mechanism for APD shortening in AnkB$^{+/-}$ myocytes (Figure 5K).

Patients with common AF display reduced ankyrin-B expression

Finally, as a first step to further investigate the linkage of AnkB with human AF in the general population, we examined the protein expression of AnkB in the right atria of patients with normal sinus rhythm versus patients with paroxysmal AF. Patients with documented paroxysmal AF displayed striking reductions in AnkB expression compared with individuals in normal sinus rhythm (Figure 6A-B, n=12 patients in sinus rhythm, n=10 pAF; $p<0.05$). Notably, we also observed a significant reduction in $Ca_v1.3$ protein expression levels in pAF samples (Figure 6C-D, n=12 patients in sinus rhythm, n=10 pAF; $p<0.05$). Together, these data provide additional data that associates reduced ankyrin-B function with human atrial disease.

Discussion

AnkB, required for the targeting and stability of critical membrane and submembrane molecules [18, 24, 25] is important for normal membrane excitability in multiple cardiac cell types [26]. The multifunctional capacity of ankyrin-B is evident in the strong link between ankyrin dysfunction and a spectrum of cardiac disorders collectively referred to as “ankyrin-B syndrome”. In this study, we identify the L-type calcium channel 1.3 (α1D) as a novel AnkB-binding partner and provide an association between decreased AnkB function and AF. Specifically, we demonstrate early-onset familial AF in human patients with an *ANK2* mis-sense mutation. AnkB$^{+/-}$ mice display similar atrial dysfunction including increased incidence of spontaneous AF episodes and enhanced susceptibility to burst-pacing induced AF. At the cellular level, ankyrin-B$^{+/-}$ atrial myocytes exhibit decreased $I_{Ca,L}$ and shortened action potential duration, both hallmarks of clinical AF.[5, 27] Underlying the reduced $I_{Ca,L}$ in AnkB$^{+/-}$ atrial myocytes, there is a selective loss of both protein expression and membrane targeting of $Ca_V1.3$, but not $Ca_V1.2$. This selective interaction is mediated by a unique motif in the C-terminal domain of $Ca_V1.3$ that is both necessary and sufficient for ankyrin-

binding. Thus, AnkB-dependent membrane targeting of $Ca_V1.3$ is required for normal atrial $I_{Ca,L}$ and atrial function. While AnkB haploinsufficiency in atrial myocytes reduces NCX and NKA currents, ankyrin-B-dependent reduction in $I_{Ca,L}$ appears primarily responsible for shortened action potential durations as suggested by computational modeling.

There is a strong association between reduced $I_{Ca,L}$ and AF.[27] While it is unclear whether $I_{Ca,L}$ dysfunction is a cause or effect of AF, there are numerous examples of AF linked to reduced $I_{Ca,L}$. Atrial tissues from human AF patients display reduced mRNA expression of L-type Ca^{2+} channels $Ca_V1.2$ and $Ca_V1.3$ in addition to an overall decrease in $I_{CA,L}$.[28, 29] In addition, patients with loss-of-function mutations in L-type Ca^{2+} channel $Ca_V1.2$ manifest complex cardiac phenotypes including AF.[30] Similarly, atrial myocytes from $Ca_v1.3^{-/-}$ mice exhibit reduced $I_{Ca,L}$, a depolarizing shift in voltage-dependent $I_{Ca,L}$ activation ($Ca_V1.3$ activates at more negative potentials than $Ca_v1.2$)[31], and increased AF susceptibility upon burst-pacing stimulation.[31, 32] Given the increased susceptibility to AF in $Ca_v1.3^{-/-}$ mice and our findings that $Ca_V1.3$ membrane targeting is regulated by a direct interaction with AnkB, it will be critical in future experiments to determine the direct role of $Ca_v1.3$-dysfunction in human *ANK2*-related atrial disease.

An intriguing finding from this study is that despite overlapping expression patterns of the L-type calcium channel alpha-subunits in atrial cells, AnkB preferentially interacts with $Ca_V1.3$ and not $Ca_V1.2$ in atrial myocytes. A second interesting observation is that $Ca_V1.3$ is expressed, albeit to a lesser extent, in membranes of $AnkB^{-/-}$ cells, suggesting that ankyrin-independent mechanisms also contribute to $Ca_V1.3$ membrane expression. These observations are consistent with L-type calcium channels interacting with a variety of signaling and scaffolding proteins that influence membrane expression. Some of the molecular mechanisms that regulate L-type calcium channel membrane expression include channel auxiliary subunits (β-subunits)[33], signaling molecules (calmodulin)[34], and scaffolding/adapter proteins (α-actinin2, A-kinase anchoring protein 79).[35, 36]

Conclusions

We propose that ankyrin-B dysfunction is associated with AF based on our findings that: 1) a loss-of-function *ANK2* mutation is associated with highly penetrant AF; 2) AnkB haplo-insufficient mice exhibit increased susceptibility to AF; 3) AnkB-deficient atrial myocytes display shortened action potentials, a hallmark of clinical AF; 4) $AnkB^{+/-}$ atrial myocytes exhibit reduced expression and membrane targeting of $Ca_v1.3$, a L-type calcium channel subunit previously associated with increased AF susceptibility[31, 32]; and 5) patients with pAF demonstrate reduced AnkB. Collectively, these findings suggest that ankyrin-B dysfunction may account for cases of monogenic AF in the general human population and that *ANK2* should be considered for familial AF screening.

Supplementary Material

Refer to Web version on PubMed Central for supplementary material.

Acknowledgments

The authors acknowledge the Heidelberg Cardiosurgeon Team and excellent technical assistance from Claudia Liebetrau in Mannheim.

Sources of Funding We acknowledge support from the NIH (HL084583, HL083422 to PJM; HL079031, HL 62494, HL70250 to MEA; HL089598, HL091947 to XHTW; HL096805 to TJH; HL092232 to SRC; Pew Scholars Trust (PJM), Gilead Sciences Research Scholars Program (TJH), W.M. Keck Foundation (XHTW), American Heart Association (NL), and Fondation Leducq Award to the Alliance for Calmodulin Kinase Signaling in Heart Disease (PJM, XHW, MEA), and Fondation Leducq Grant to the European-North American Atrial Fibrillation Research Alliance (DD).

References

1. Damani SB, Topol EJ. Molecular genetics of atrial fibrillation. Genome medicine. 2009; 1:54. [PubMed: 19490585]
2. Furberg CD, Psaty BM, Manolio TA, Gardin JM, Smith VE, Rautaharju PM. Prevalence of atrial fibrillation in elderly subjects (the cardiovascular health study). The American journal of cardiology. 1994; 74:236–241. [PubMed: 8037127]
3. Wolf PA, Abbott RD, Kannel WB. Atrial fibrillation as an independent risk factor for stroke: The framingham study. Stroke; a journal of cerebral circulation. 1991; 22:983–988.
4. Miyasaka Y, Barnes ME, Gersh BJ, Cha SS, Bailey KR, Abhayaratna WP, Seward JB, Tsang TS. Secular trends in incidence of atrial fibrillation in olmsted county, minnesota, 1980 to 2000, and implications on the projections for future prevalence. Circulation. 2006; 114:119–125. [PubMed: 16818816]
5. Nattel S, Burstein B, Dobrev D. Atrial remodeling and atrial fibrillation: Mechanisms and implications. Circ Arrhythm Electrophysiol. 2008; 1:62–73. [PubMed: 19808395]
6. Ellinor PT, Petrov-Kondratov VI, Zakharova E, Nam EG, MacRae CA. Potassium channel gene mutations rarely cause atrial fibrillation. BMC Med Genet. 2006; 7:70. [PubMed: 16887036]
7. Cunha SR, Mohler PJ. Ankyrin protein networks in membrane formation and stabilization. J Cell Mol Med. 2009; 3:4364–4376. [PubMed: 19840192]
8. Kline CF, Kurata HT, Hund TJ, Cunha SR, Koval OM, Wright PJ, Christensen M, Anderson ME, Nichols CG, Mohler PJ. Dual role of katp channel c-terminal motif in membrane targeting and metabolic regulation. Proc Natl Acad Sci U S A. 2009; 106:16669–16674. [PubMed: 19805355]
9. Mohler PJ, Schott JJ, Gramolini AO, Dilly KW, Guatimosim S, duBell WH, Song LS, Haurogne K, Kyndt F, Ali ME, Rogers TB, Lederer WJ, Escande D, Le Marec H, Bennett V. Ankyrin-b mutation causes type 4 long-qt cardiac arrhythmia and sudden cardiac death. Nature. 2003; 421:634–639. [PubMed: 12571597]
10. Scotland P, Zhou D, Benveniste H, Bennett V. Nervous system defects of ankyrinb (−/−) mice suggest functional overlap between the cell adhesion molecule l1 and 440-kd ankyrinb in premyelinated axons. J Cell Biol. 1998; 143:1305–1315. [PubMed: 9832558]
11. Mohler PJ, Davis JQ, Bennett V. Ankyrin-b coordinates the na/k atpase, na/ca exchanger, and insp(3) receptor in a cardiac t-tubule/sr microdomain. PLoS Biol. 2005; 3:e423. [PubMed: 16292983]
12. Le Scouarnec S, Bhasin N, Vieyres C, Hund TJ, Cunha SR, Koval O, Marionneau C, Chen B, Wu Y, Demolombe S, Song LS, Le Marec H, Probst V, Schott JJ, Anderson ME, Mohler PJ. Dysfunction in ankyrin-b-dependent ion channel and transporter targeting causes human sinus node disease. Proc Natl Acad Sci U S A. 2008; 105:15617–15622. [PubMed: 18832177]
13. Mohler PJ, Splawski I, Napolitano C, Bottelli G, Sharpe L, Timothy K, Priori SG, Keating MT, Bennett V. A cardiac arrhythmia syndrome caused by loss of ankyrin-b function. Proc Natl Acad Sci U S A. 2004; 101:9137–9142. [PubMed: 15178757]
14. Mohler PJ, Le Scouarnec S, Denjoy I, Lowe JS, Guicheney P, Caron L, Driskell IM, Schott JJ, Norris K, Leenhardt A, Kim RB, Escande D, Roden DM. Defining the cellular phenotype of “ankyrin-b syndrome” variants: Human ank2 variants associated with clinical phenotypes display a spectrum of activities in cardiomyocytes. Circulation. 2007; 115:432–441. [PubMed: 17242276]
15. Chelu MG, Sarma S, Sood S, Wang S, van Oort RJ, Skapura DG, Li N, Santonastasi M, Muller FU, Schmitz W, Schotten U, Anderson ME, Valderrabano M, Dobrev D, Wehrens XH. Calmodulin kinase ii-mediated sarcoplasmic reticulum ca2+ leak promotes atrial fibrillation in mice. J Clin Invest. 2009; 119:1940–1951. [PubMed: 19603549]
16. Mangoni ME, Couette B, Bourinet E, Platzer J, Reimer D, Striessnig J, Nargeot J. Functional role of l-type cav1.3 ca2+ channels in cardiac pacemaker activity. Proc Natl Acad Sci U S A. 2003; 100:5543–5548. [PubMed: 12700358]
17. Dobrev D, Graf E, Wettwer E, Himmel HM, Hala O, Doerfel C, Christ T, Schuler S, Ravens U. Molecular basis of downregulation of g-protein-coupled inward rectifying k(+) current (i(k,ach) in chronic human atrial fibrillation: Decrease in girk4 mrna correlates with reduced i(k,ach) and

muscarinic receptor-mediated shortening of action potentials. Circulation. 2001; 104:2551–2557. [PubMed: 11714649]

18. Cunha SR, Bhasin N, Mohler PJ. Targeting and stability of na/ca exchanger 1 in cardiomyocytes requires direct interaction with the membrane adaptor ankyrin-b. J Biol Chem. 2007; 282:4875–4883. [PubMed: 17178715]
19. Lowe JS, Palygin O, Bhasin N, Hund TJ, Boyden PA, Shibata E, Anderson ME, Mohler PJ. Voltage-gated nav channel targeting in the heart requires an ankyrin-g dependent cellular pathway. J Cell Biol. 2008; 180:173–186. [PubMed: 18180363]
20. Garrido JJ, Giraud P, Carlier E, Fernandes F, Moussif A, Fache MP, Debanne D, Dargent B. A targeting motif involved in sodium channel clustering at the axonal initial segment. Science. 2003; 300:2091–2094. [PubMed: 12829783]
21. Mohler PJ, Rivolta I, Napolitano C, Lemaillet G, Lambert S, Priori SG, Bennett V. Nav1.5 e1053k mutation causing brugada syndrome blocks binding to ankyrin-g and expression of nav1.5 on the surface of cardiomyocytes. Proc Natl Acad Sci U S A. 2004; 101:17533–17538. [PubMed: 15579534]
22. Mohler PJ, Healy JA, Xue H, Puca AA, Kline CF, Allingham R Rand, Kranias EG, Rockman HA, Bennett V. Ankyrin-b syndrome: Enhanced cardiac function balanced by risk of cardiac death and premature senescence. PLoS ONE. 2007; 2:e1051. [PubMed: 17940615]
23. Courtemanche M, Ramirez RJ, Nattel S. Ionic mechanisms underlying human atrial action potential properties: Insights from a mathematical model. Am J Physiol. 1998; 275:H301–321. [PubMed: 9688927]
24. Bhasin N, Cunha SR, Mudannayake M, Gigena MS, Rogers TB, Mohler PJ. Molecular basis for pp2a regulatory subunit b56{alpha} targeting in cardiomyocytes. Am J Physiol Heart Circ Physiol. 2007; 293:H109–119. [PubMed: 17416611]
25. Cunha SR, Mohler PJ. Obscurin targets ankyrin-b and protein phosphatase 2a to the cardiac m-line. J Biol Chem. 2008; 283:31968–31980. [PubMed: 18782775]
26. Mohler PJ, Bennett V. Defects in ankyrin-based cellular pathways in metazoan physiology. Front Biosci. 2005; 10:2832–2840. [PubMed: 15970537]
27. Yue L, Feng J, Gaspo R, Li GR, Wang Z, Nattel S. Ionic remodeling underlying action potential changes in a canine model of atrial fibrillation. Circ Res. 1997; 81:512–525. [PubMed: 9314832]
28. Christ T, Boknik P, Wohrl S, Wettwer E, Graf EM, Bosch RF, Knaut M, Schmitz W, Ravens U, Dobrev D. L-type ca2+ current downregulation in chronic human atrial fibrillation is associated with increased activity of protein phosphatases. Circulation. 2004; 110:2651–2657. [PubMed: 15492323]
29. Gaborit N, Steenman M, Lamirault G, Le Meur N, Le Bouter S, Lande G, Leger J, Charpentier F, Christ T, Dobrev D, Escande D, Nattel S, Demolombe S. Human atrial ion channel and transporter subunit gene-expression remodeling associated with valvular heart disease and atrial fibrillation. Circulation. 2005; 112:471–481. [PubMed: 16027256]
30. Antzelevitch C, Pollevick GD, Cordeiro JM, Casis O, Sanguinetti MC, Aizawa Y, Guerchicoff A, Pfeiffer R, Oliva A, Wollnik B, Gelber P, Bonaros EP Jr. Burashnikov E, Wu Y, Sargent JD, Schickel S, Oberheiden R, Bhatia A, Hsu LF, Haissaguerre M, Schimpf R, Borggrefe M, Wolpert C. Loss-of-function mutations in the cardiac calcium channel underlie a new clinical entity characterized by st-segment elevation, short qt intervals, and sudden cardiac death. Circulation. 2007; 115:442–449. [PubMed: 17224476]
31. Zhang Z, He Y, Tuteja D, Xu D, Timofeyev V, Zhang Q, Glatter KA, Xu Y, Shin HS, Low R, Chiamvimonvat N. Functional roles of cav1.3(alpha1d) calcium channels in atria: Insights gained from gene-targeted null mutant mice. Circulation. 2005; 112:1936–1944. [PubMed: 16172271]
32. Mancarella S, Yue Y, Karnabi E, Qu Y, El-Sherif N, Boutjdir M. Impaired ca2+ homeostasis is associated with atrial fibrillation in the alpha1d l-type ca2+ channel ko mouse. Am J Physiol Heart Circ Physiol. 2008; 295:H2017–2024. [PubMed: 18790836]
33. Obermair GJ, Schlick B, Di Biase V, Subramanyam P, Gebhart M, Baumgartner S, Flucher BE. Reciprocal interactions regulate targeting of calcium channel beta subunits and membrane expression of alpha1 subunits in cultured hippocampal neurons. J Biol Chem. 2010; 285:5776–5791. [PubMed: 19996312]

34. Wang HG, George MS, Kim J, Wang C, Pitt GS. Ca2+/calmodulin regulates trafficking of ca(v)1.2 ca2+ channels in cultured hippocampal neurons. J Neurosci. 2007; 27:9086–9093. [PubMed: 17715345]

35. Sadeghi A, Doyle AD, Johnson BD. Regulation of the cardiac l-type ca2+ channel by the actin-binding proteins alpha-actinin and dystrophin. Am J Physiol Cell Physiol. 2002; 282:C1502–1511. [PubMed: 11997265]

36. Altier C, Dubel SJ, Barrere C, Jarvis SE, Stotz SC, Spaetgens RL, Scott JD, Cornet V, De Waard M, Zamponi GW, Nargeot J, Bourinet E. Trafficking of l-type calcium channels mediated by the postsynaptic scaffolding protein akap79. J Biol Chem. 2002; 277:33598–33603. [PubMed: 12114507]

Atrial fibrillation (AF) is the most prevalent sustained arrhythmia in clinical practice. In fact, in the US alone, AF is present in >two million individuals. Despite the high incidence of AF in the population, surprisingly little is known regarding the molecular mechanisms underlying this complex disease. Ankyrin proteins target and stabilize proteins at specialized membrane domains. Notably, dysfunction in ankyrin- and ankyrin-associated pathways has been linked with disorders including spherocytosis, spinocerebellar ataxia, diabetes, neurological deficits, and cardiac arrhythmias. Nearly a decade ago, ankyrin-B (*ANK2*) was discovered as a critical component of heart, and work in humans and mice has implicated ankyrin-B as critical for cardiac function. In fact, human *ANK2* loss-of-function variants are associated with potentially fatal ventricular arrhythmias. Here, we demonstrate the importance of ankyrin-B for atrial function and identify an association between ankyrin-B dysfunction and AF. Individuals harboring *ANK2*-variants display AF and these phenotypes are reproduced in mice deficient in ankyrin-B. Ankyrin-B is expressed in the atria and ankyrin-$B^{+/-}$ myocytes display shortened action potentials, a hallmark of AF, and decreased L-type calcium channel current ($I_{Ca,L}$). We show that $Ca_v1.3$, responsible for one component of $I_{Ca,L}$ in atria, is a novel ankyrin-binding partner and that $Ca_v1.3$ expression/activity is reduced in ankyrin-deficient atrial myocytes. Finally, ankyrin-B is reduced in atrial samples from human AF patients, further supporting the role of ankyrin-B in normal atrial function. Together, our work implicates ankyrin-B as a surprising, yet critical component of atrial excitability, and supports the role of atypical myocyte proteins in disease pathogenesis.

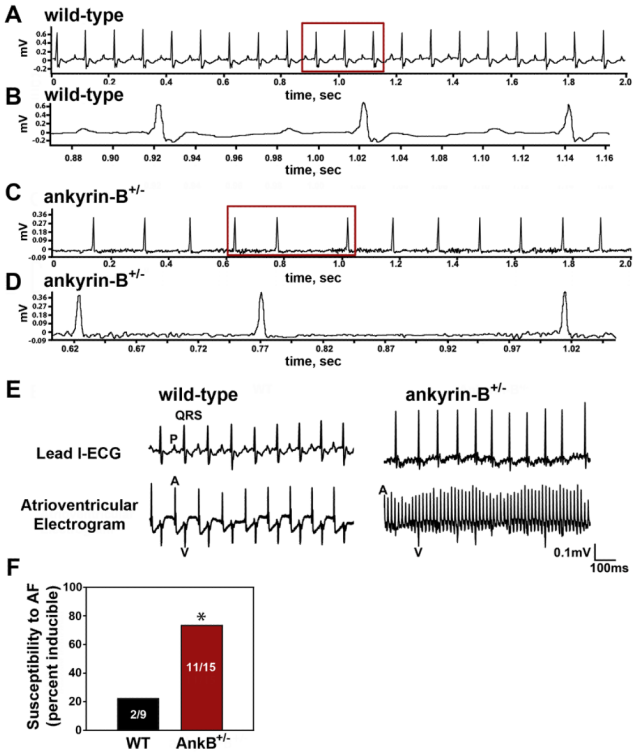

Figure 1. Ankyrin-deficient mice display atrial dysfunction and atrial fibrillation (AF) inducibility

A-D, Conscious ECGs of WT **(A-B)** and AnkB$^{+/-}$ mice **(C-D)** recorded by telemetry. WT mice show normal sinus rhythm whereas AnkB$^{+/-}$ mice display spontaneous bradycardia with erratic atrial activity, including absence of discreet P waves and variable ventricular responses indicative of spontaneous AF. B and D represent red magnified areas of A and C. **E**, Simultaneous surface ECG (top) and atrioventricular electrogram recording (bottom) in WT (left) and AnkB$^{+/-}$ mice (right). *Top*, Lead I ECG from WT and AnkB$^{+/-}$ mice shows rapid atrial electrical activity and the variability in RR interval in AnkB$^{+/-}$ mouse compared to the WT mouse. **F,** Incidence of AF in WT and AnkB$^{+/-}$ mice during burst-pacing. While WT mice displayed low incidence of AF (2/9 mice), AnkB$^{+/-}$ mice were highly susceptible to AF induction (11/15 *$p<0.05$ for AF susceptibility in WT vs. AnkB$^{+/-}$ mice).

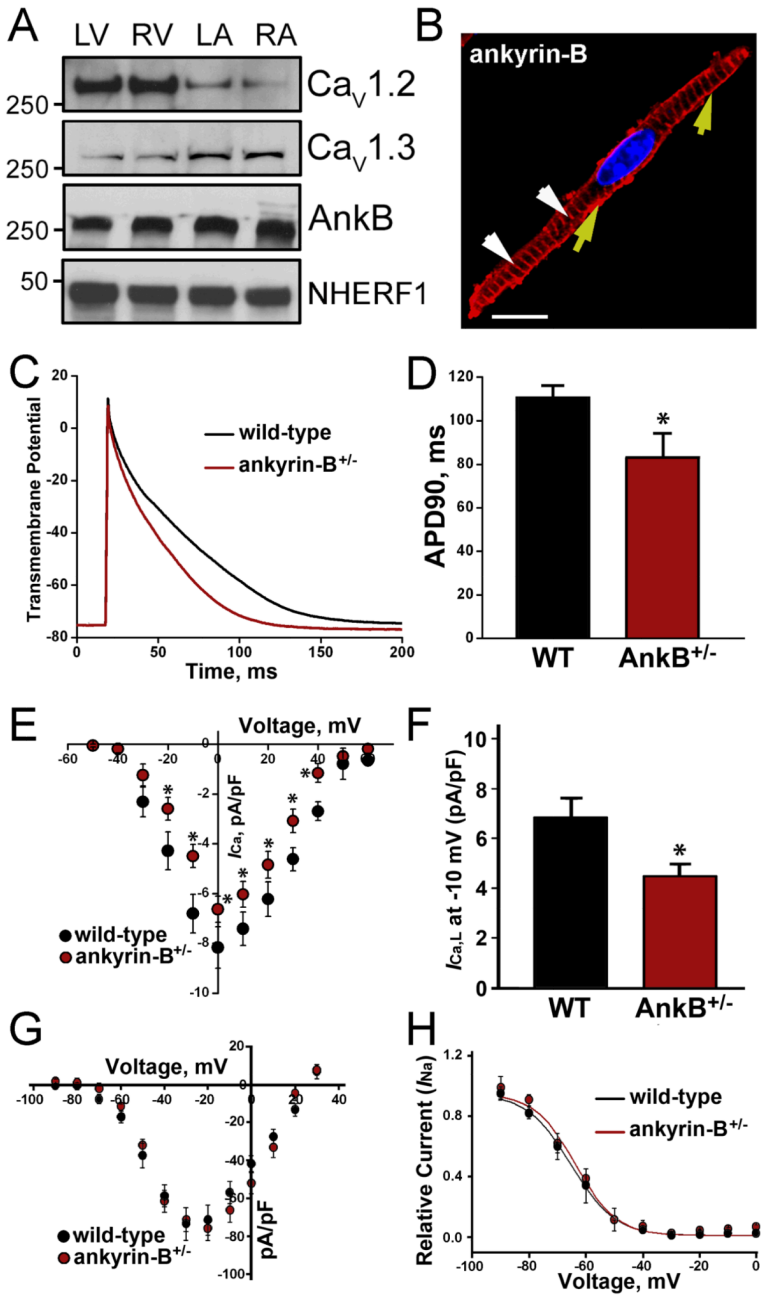

Figure 2. Ankyrin-B$^{+/-}$ atrial myocytes display reduced APD and decreased $I_{Ca,L}$

A, AnkB is expressed in human right and left atria (RA, LA), as well as right and left ventricles (RV, LV). $Ca_V1.2$ expression is greater in ventricles than atria, while $Ca_V1.3$ expression is greater in atria than ventricles. NHERF1 expression demonstrates equal loading between the samples. **B**, Localization of AnkB in a single mouse atrial myocyte. Note that AnkB is expressed at both the sarcolemma (yellow arrows) as well as M-line domains (white arrows). Scale bar equals 10 microns. **C-D**, AnkB$^{+/-}$ atrial myocytes display reduced action potential duration (APD90 at 22°C; n=7 WT, n=8 AnkB$^{+/-}$, $p<0.05$). **E-F**, AnkB$^{+/-}$ atrial myocytes display reduced $I_{Ca,L}$ compared with WT atrial myocytes (n=7

WT, n=8 AnkB$^{+/-}$, p<0.05). **G-H**, WT and AnkB$^{+/-}$ atrial myocytes display no difference in I_{Na} (n=7 WT, n=8 AnkB$^{+/-}$, p<0.05).

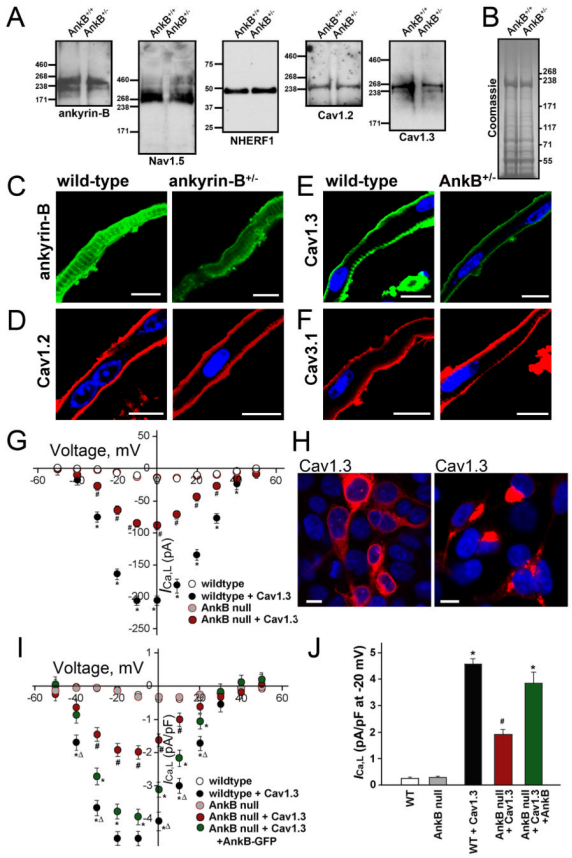

Figure 3. Reduced $Ca_V1.3$ expression and targeting in ankyrin-$B^{+/-}$ atria

A, Immunoblots to evaluate expression of AnkB, $Na_V1.5$, NHERF1, $Ca_V1.2$, and $Ca_V1.3$ protein in WT and ankyrin-$B^{+/-}$ mouse atria. Note reduced protein expression of AnkB and $Ca_V1.3$ in $AnkB^{+/-}$ atria compared to WT atria (n=3, $p<0.05$). No change was detected in the protein expression of $Ca_V1.2$, $Na_V1.5$, and NHERF1 between WT and ankyrin-$B^{+/-}$ atria (n=3, N.S.). **B**, Coomassie Blue stain demonstrating equal loading of protein lysates from WT and ankyrin-$B^{+/-}$ atria. **C-F**, Immunolocalization of AnkB (**C**), $Ca_v1.2$ (**D**), $Ca_v1.3$ (**E**), and $Ca_v3.1$ (**F**) in WT (left panel) and $AnkB^{+/-}$ atrial myocytes (right panel). Note decreased membrane targeting of $Ca_v1.3$, but not other membrane proteins ($Ca_v1.2$, $Ca_v3.1$) in $AnkB^{+/-}$ atrial myocytes (n=5 WT, n=6 $AnkB^{+/-}$; $p<0.05$ for $Ca_v1.3$). Scale bar equals 10 microns. **G-J,** Ankyrin-B expression is required for normal atrial myocyte $I_{Ca,L}$. **G**, $I_{Ca,L}$ in WT and ankyrin-$B^{-/-}$ primary cells with and without exogenous $Ca_v1.3$. Note that $AnkB^{-/-}$ cardiac fibroblasts expressing $Ca_v1.3$ display significant reductions in $I_{Ca,L}$ compared with WT fibroblasts expressing identical $Ca_v1.3$ cDNAs (n=9 WT, n=7 $AnkB^{+/-}$). * notes $p<0.05$ for black vs. red symbols; # notes $p<0.05$ for red symbols vs. untransfected cells. **H**, Decreased membrane expression of $Ca_v1.3$ (red) in wild-type (left) versus AnkB-deficient (right) primary cells (scale bar represents 10 microns, blue staining represents nuclei). **I-J**, Reduced $I_{Ca,L}$ in ankyrin-B null fibroblasts is rescued to normal by co-expression of GFP-tagged AnkB. * notes $p<0.05$ for black and green vs. red symbols; # notes $p<0.05$ for red symbols vs. untransfected cells; Δ represents $p<0.05$ between black and green symbols (n=8/group).

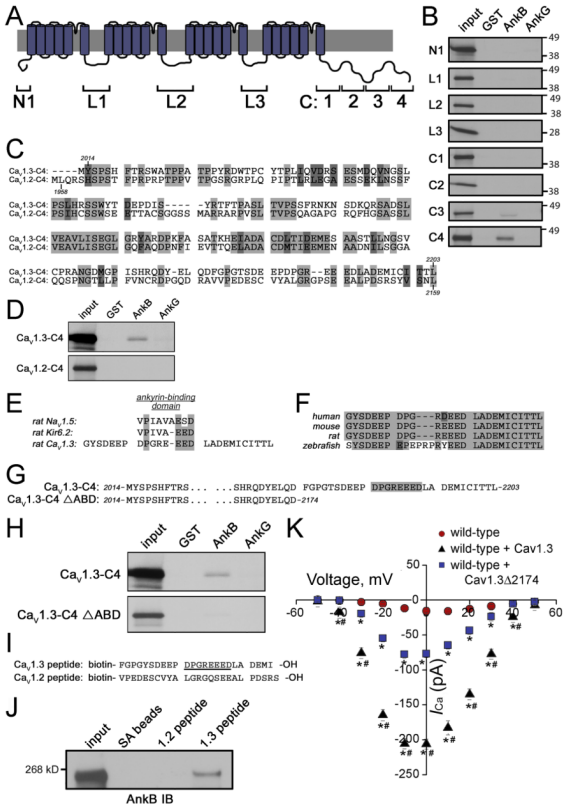

Figure 4. Ankyrin-B directly associates with Ca$_V$1.3. A, Schematic representation of rat Ca$_V$1.3 and intracellular domains for *in vitro* binding assays

Intracellular domains correspond to amino acids N1: 1-127, L1: 406-583, L2: 811-946, L3: 1207-1263, C1: 1504-1670, C2: 1671-1853, C3: 1854-2019, and C4: 2014-2202. **B**, *In vitro* binding assays between Ca$_V$1.3 intracellular domains and ankyrin membrane-binding domains. Note the membrane-binding domain of AnkB, but not ankyrin-G, binds to Ca$_V$1.3 C4 representing the terminal ~200 amino acids. **C**, Amino acid alignment of the terminal ~200 amino acids of Ca$_V$1.3 and Ca$_V$1.2. Identical amino acids are boxed in light gray, while similar amino acids are boxed in dark gray. **D**, *In vitro* binding assays of AnkB membrane-binding domain with the corresponding C4 regions of Ca$_V$1.3 and Ca$_V$1.2. Note that AnkB selectively interacts with Ca$_V$1.3 C4. **E**, Amino acid alignment of known ankyrin-binding domains in Na$_V$1.5 and Kir6.2 with the ankyrin-binding domain in the terminal 26 amino acids of Ca$_V$1.3. **F**, High amino acid conservation is observed in Ca$_V$1.3 ankyrin-binding domains across species. **G**, Amino acid sequences of full-length Ca$_V$1.3-C4 and Ca$_V$1.3-C4 lacking the terminal 29 amino acids including the ankyrin-binding domain (Ca$_V$1.3-C4 ΔABD). **H**, *In vitro* binding assays of AnkB membrane-binding domain with Ca$_V$1.3-C4 and Ca$_V$1.3-C4 ΔABD. Note that AnkB does not bind to Ca$_V$1.3-C4 ΔABD (experiments were done in parallel with those in D). **I**, Amino acid sequences of biotinylated peptides of the terminal ~25 residues of Ca$_V$1.3 and Ca$_V$1.2. **J**, Immunoprecipitation of ankyrin-B with the biotinylated Ca$_V$1.3 peptide, but not with the corresponding Ca$_V$1.2 peptide. **K,** Compared to primary cardiac fibroblasts expressing WT Ca$_V$1.3, primary cardiac fibroblasts expressing Ca$_V$1.3 lacking the AnkB-binding motif display reduced $I_{Ca,L}$. * represent $p<0.05$ compared with red symbols; # represents $p<0.05$ of triangles compared with squares (n=7/group).

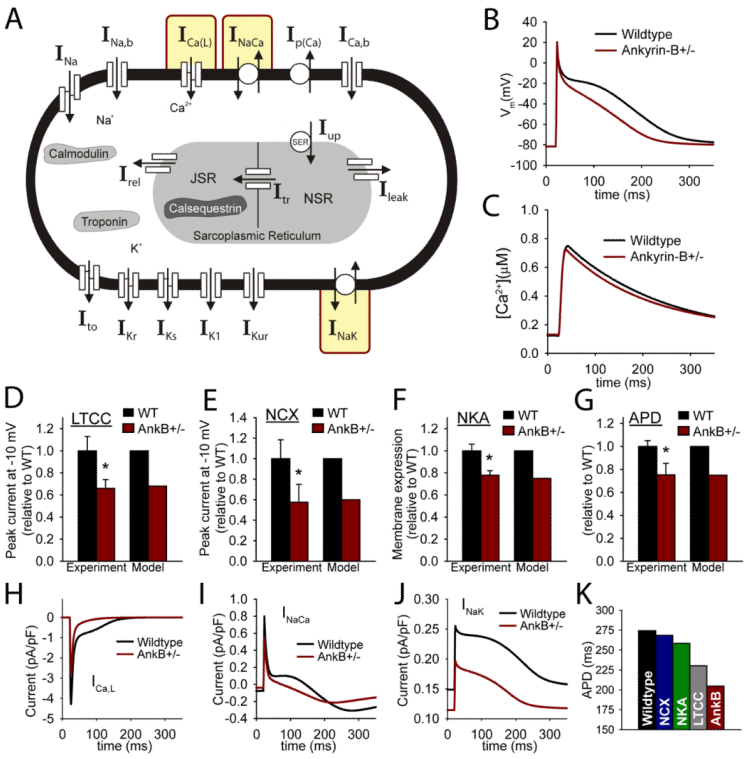

Figure 5. Computational analysis of mechanism for action potential remodeling in ankyrin-B$^{+/-}$ atrial myocytes and reduced atrial ankyrin-B expression in AF patients

A, Schematic of mathematical model used to simulate the atrial action potential. L-type Ca^{2+} current ($I_{Ca,L}$), NCX current (I_{NaCa}) and NKA current (I_{NaK}) (*yellow boxes*) were altered based on experimental measurements to create the model of the AnkB$^{+/-}$ atrial myocyte. Simulated action potentials (**B**) and calcium transients (**C**) from WT and AnkB$^{+/-}$ atrial myocytes. Consistent with experimental data, the AnkB$^{+/-}$ model shows decreased **(D,H)** $I_{Ca(L)}$, **(E,I)** I_{NaCa}, and **(F,J)** I_{NaK}, and action potential duration at 90% of repolarization (APD) (AnkB$^{+/-}$ 90 APD 75% of WT in model compared to 75±10% in experiment) (**G**). **K,** $I_{Ca.L}$, I_{NaCa} and I_{NaK} were altered independently to determine the mechanism for APD shortening in AnkB$^{+/-}$ atrial myocytes. Decreasing $I_{Ca,L}$ alone shortened APD by nearly the same amount as observed in the AnkB$^{+/-}$ model.

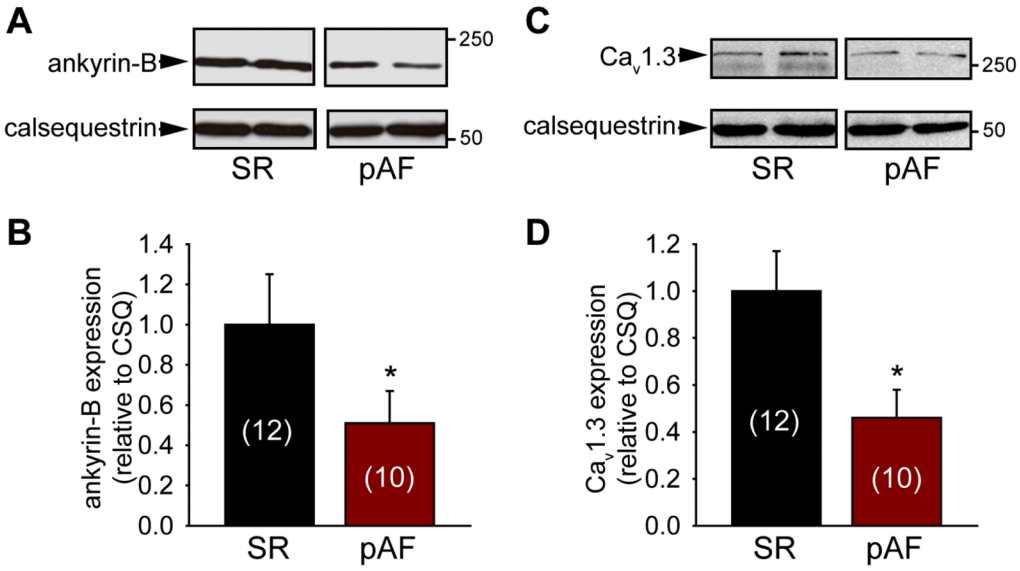

Figure 6. Decreased ankyrin-B and $Ca_V1.3$ protein expression in atria from human pAF patients

A-D, ankyrin-B and $Ca_V1.3$ are decreased in right atria of patients with documented paroxysmal AF compared to individuals in normal sinus rhythm (n=10 AF, n=12 sinus rhythm, $p<0.05$). Expression levels are shown relative to calsequestrin expression to correct for potential minor differences in protein loading.